The mineralogy, petrology, and composition of anomalous eucrite Emmaville

The Meteoritical Society

Meteoritics & Planetary Science 52, Nr 4, 656–668 (2017)
doi: 10.1111/maps.12818

The mineralogy, petrology, and composition of anomalous eucrite Emmaville

T. J. BARRETT[1,*], D. W. MITTLEFEHLDT[2], R. C. GREENWOOD[1], B. L. A. CHARLIER[1], S. J. HAMMOND[1], D. K. ROSS[2,3], M. ANAND[1,4], I. A. FRANCHI[1], F. A. J. ABERNETHY[1], and M. M. GRADY[1]

[1]School of Physical Sciences, The Open University, Walton Hall, Milton Keynes MK7 6AA, UK
[2]Astromaterials Research Office, NASA Johnson Space Center, Houston, Texas 77058, USA
[3]UTEP and Jacobs Technology, 2224 Bay Area Blvd, Houston, Texas 77058, USA
[4]Department of Earth Sciences, Natural History Museum, London SW7 5BD, UK
[*]Corresponding author. E-mail: thomas.barrett@open.ac.uk

(Received 18 March 2016; revision accepted 17 November 2016)

Abstract–The Emmaville eucrite is a relatively poorly studied basaltic achondrite with an anomalous oxygen isotope signature. In this study, we report comprehensive mineralogical, petrographic, and geochemical data from Emmaville in order to understand its petrogenesis and relationship with the basaltic eucrites. Emmaville is an unusually fine-grained, hornfelsic-textured metabasalt with pervasive impact melt veins and mineral compositions similar to those of typical basaltic eucrites. The major and trace element bulk composition of Emmaville is also typical of a basaltic eucrite. Three separated individual lithologies were also analyzed for O isotopes; a dark gray fraction (E1), a shocked lithology (E2), and a lighter gray portion (E3). Fractions E1 and E2 shared similar O isotope compositions to the bulk sample (E-B), whereas the lighter gray portion (E3) is slightly elevated in $\Delta^{17}O$ and significantly elevated in $\delta^{18}O$ compared to bulk. No evidence for any exogenous material is observed in the thin sections, coupled with the striking compositional similarity to typical basaltic eucrites, appears to preclude a simple impact-mixing hypothesis. The O-isotopes of Emmaville are similar to those of Bunburra Rockhole, A-881394, and EET 92023, and thus distinct from the majority of the HEDs, despite having similarities in petrology, mineral, and bulk compositions. It would, therefore, seem plausible that all four of these samples are derived from a single HED-like parent body that is isotopically distinct from that of the HEDs (Vesta) but similar in composition.

INTRODUCTION

It has long been known that certain basaltic achondrites share similarities with eucrites. These eucrite-like achondrites have distinct isotopic compositions and petrologic characteristics indicative of formation on a separate parent body from the HED clan (e.g., Ibitira, Northwest Africa [NWA] 011; Yamaguchi et al. 2002; Wiechert et al. 2004; Floss et al. 2005; Greenwood et al. 2005; Mittlefehldt 2005). Others show smaller isotopic variations but are otherwise petrologically and compositionally indistinguishable from basaltic eucrites, such as Pasamonte (Wiechert et al. 2004; Greenwood et al. 2005; Scott et al. 2009). Studying anomalous eucrites allows us to more completely understand the number of parent asteroids represented by eucrite-like basalts as well as further constrain the chemical and isotopic diversity present within the HED suite. The Emmaville eucrite is a fall and has a $\Delta^{17}O$ value of -0.137 ± 0.024 ‰ (1σ) (Greenwood et al. 2013), substantially different from the eucrite mean of -0.246 ± 0.014 ‰ (2σ) (Greenwood et al. 2014), but similar to those of Asuka 881394 (A-881394; Scott et al. 2009) and Bunburra Rockhole (Bland et al. 2009; Fig. 1).

Currently little data exist for Emmaville in terms of petrology or bulk composition (Morgan and Lovering 1973; Mason 1974; Stolper 1977; Yamaguchi et al. 1996). In this study, we present a comprehensive examination of the petrology, mineral compositions,

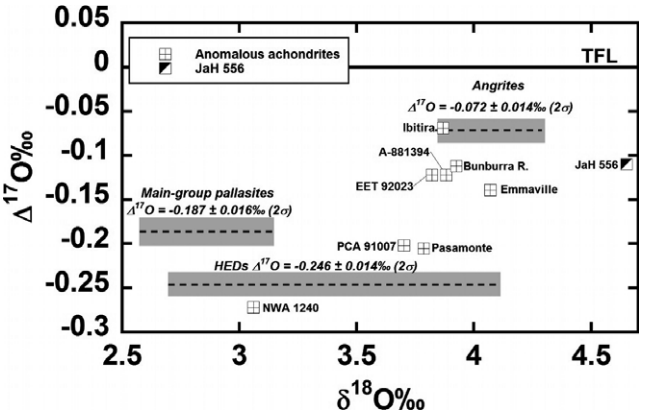

Fig. 1. Oxygen isotope composition of anomalous achondrites shown in relation to HEDs, angrites, and main-group pallasites. Data compiled from Greenwood et al. (2005, 2012, 2013, 2016); Scott et al. (2009); Janots et al. (2012).

and major and trace element abundances along with O isotopic data to address three possibilities that 1) the HED parent body is not as well homogenized as was previously considered, 2) Emmaville is from a separate parent body that generated eucrite-like basalts, or 3) mixing of impactor material with contrasting O isotopic composition into Emmaville affected its composition.

SAMPLES AND ANALYTICAL APPROACH

Analyses were conducted on two polished thin sections of Emmaville (Smithsonian Institute, USNM 5755 1; Natural History Museum, London, P293), using the JEOL8530F field emission election probe microanalyzer (EPMA) at the NASA Johnson Space Center. Beam conditions included an accelerating voltage of 20 kV, and a beam current of 40 nA for pyroxene, with a spot size set to ~0.01 μm (giving an excitation volume of ~1 μm^3). These beam conditions and the counting times used are those of Mittlefehldt (2005) and result in greater precision of Fe/Mn ratios than commonly used EPMA protocols. Plagioclase was analyzed with a 15 kV, 20 nA beam, and 3 μm spot size. Modal abundances were calculated using the pixel histograms in the free software ImageJ® on a number (n = 20) of high-quality back scatter electron (BSE) images which were then averaged to achieve a representative sample of the section (~5.84 mm^2).

Raman Spectroscopy

Raman spectroscopy was conducted on a Horiba Jobin Yvon LabRam HR at the Open University. A 514.53 nm laser with a laser power of 1.45–1.71 mW and spot size of ~2 μm was used for analysis and standardized with a Si chip. Hole and slit settings were 300 μm and 150 μm, respectively. Analyses consisted of two 10 s collections using a 50 × objective lens and a 600 grooves per mm grating, giving a spectral range of ~0–1900 wave numbers. Three maps were taken ranging in size from 29 × 44 μm to 91 × 135 μm with separations ranging from 2–5 μm. A linear baseline was used for data correction.

Major, Minor, and Trace Element Analysis

For bulk major and trace element analysis powdered samples were weighed into clean 7 ml Savillex™ beakers. Sample amounts ranged from 13.57 mg (Ibitira) to 113.30 mg (Tirhert). Sample dissolution was achieved using standard HF-HNO_3 digestion techniques (Rogers et al. 2006), followed by 1000-fold dilution for analysis in 2% HNO_3. Major elements were analyzed using a Teledyne-Leemans Prodigy high-dispersion ICP-OES (inductively coupled plasma-optical emission spectrometer), operating in axial view, and standards were prepared using a 1000 ppm certified multielement standard from Fisher Scientific. Trace elements were determined on the same solutions using an Agilent 7000a ICP-MS (inductively coupled plasma-mass spectrometer). Both instruments are located at the Open University.

The ICP-MS concentration calibrations were carried out using stock digestions of BHVO-2-, DNC-1-, AGV-1-, and W2-certified rock standards. Instrumental drift was corrected for by measuring a "monitor block" consisting of one basaltic reference standard (BIR-1), one unknown (Tirhert), and a blank solution of 2% HNO_3 after every five unknowns. Oxides (measured as CeO/Ce in the tune solution) are kept to a minimum, usually at <0.3%, and doubly charged species (Ce^{++}/Ce^{+}) at <1.0% and masses used were chosen as they are free of isobaric interferences. The average and relative standard deviation of the drift-corrected unknown in the monitor block was used to determine the precision of the measurements. For elements lighter than Rb, the relative standard deviation (1σ, n = 4) of Tirhert was <5.3%; elements heavier than Rb typically have uncertainties of much less than 4.1% (RSD 1σ). Th and U yielded slightly higher uncertainties at 5.4% and 7.3% (both 1σ), respectively. The majority of values for the average trace element data of BIR-1 agree to be better than ±10% when compared with those reported by Eggins et al. (1997) for the same rock standards, and we use this as our estimate of accuracy. Two elements, however (Hf and Rb), deviate by up to 12.2% from the Eggins et al. (1997) values. The measured and average standard values can be found in Data S1 in supporting information. A total

procedural blank was run and measured at the same time as the unknowns, as blank levels were insignificant, no correction was required.

Oxygen Isotopic Analysis: Sample Preparation and Analytical Procedures

Similar to many eucrites, Emmaville shows evidence of brecciation and the development of shock melt veins. In order to verify whether Emmaville is isotopically homogeneous, or if the different lithologies preserve distinct oxygen isotope compositions, we attempted to separate the various lithological fractions. An approximately 400 mg fusion-crusted chip (removed from the single fragment analyzed by Greenwood et al. 2013, 2016) was gently crushed in an agate mortar and various fractions were hand-picked with the aid of a binocular microscope. Three distinct fractions were separated from Emmaville for the current study: E1, a relatively homogeneous gray-colored lithology which was free of shock melt veins; E2, material containing a relatively high proportion of dark fine-grained shock melt veins; and E3, a fine-grained light-colored fraction.

Oxygen isotopic analysis was undertaken at the Open University using a modified version of the infrared laser-assisted fluorination system described by Miller et al. (1999) and the details of which can be found in Greenwood et al. (2015).

An estimate of the present level of precision of the Open University system is provided by 39 analyses of our internal obsidian standard undertaken during six separate sessions by Greenwood et al. (2015), which gave the following combined results: $\pm 0.052‰$ for $\delta^{17}O$; $\pm 0.093‰$ for $\delta^{18}O$; $\pm 0.017‰$ for $\Delta^{17}O$ (2σ). The precision (2σ) quoted for individual meteorite samples is based on replicate analyses.

Oxygen isotopic analyses are reported in standard δ notation, where $\delta^{18}O$ has been calculated as:

$$\delta^{18}O = [(^{18}O/^{16}O)_{sample}/(^{18}O/^{16}O)_{ref} - 1] \times 1000(‰)$$

$$\delta^{17}O = [(^{17}O/^{16}O)_{sample}/(^{17}O/^{16}O)_{ref} - 1] \times 1000(‰)$$

The reference being VSMOW: Vienna Standard Mean Ocean Water. $\Delta^{17}O$, which represents the deviation from the terrestrial fractionation line, has been calculated using the linearized format of Miller (2002):

$$\Delta^{17}O = 1000\ln(1 + \delta^{17}O/1000) - \lambda 1000\ln(1 + \delta^{18}O/1000)$$

where $\lambda = 0.5247$ (Miller et al. 1999; Miller 2002).

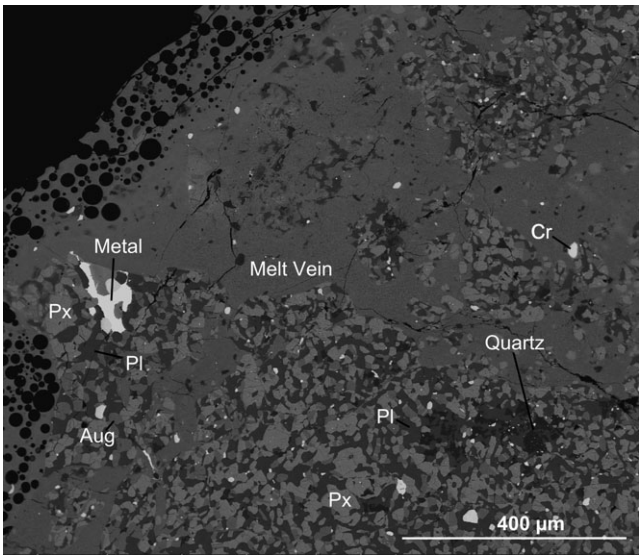

Fig. 2. Backscattered electron (BSE) image of Emmaville showing melt veins and fusion crust. Px = pyroxene, Aug = augite, Pl = plagioclase, Cr = chromite.

RESULTS

Mineralogy

Emmaville is an unusually fine-grained (<60 μm compared to the 50–100 μm grain size typical of fine-grained basaltic eucrites, for example, Mayne et al. 2009) hornfelsic-textured metabasalt (Fig. 2). The mineralogy mainly comprises low-Ca pyroxene (23.3% modal abundance), high-Ca pyroxene (21.1%), plagioclase (38.1%), and a silica phase (8.9%), identified here as quartz by Raman spectroscopy (see Data S2 in supporting information). Minor phases include ilmenite, chromite (combined oxide modal abundance 1.3%), troilite (trace), and melt veins (7.3%). During our detailed petrographic analysis only two <10 μm zircon grains and two Ni-poor metal grains were observed. Average mineral compositions are given in Table 1.

Pyroxene and plagioclase grains are typically 10–30 μm across, but some regions have noticeably coarser grain size of ~100 μm in the longest dimension. Emmaville also contains ~100 μm wide melt veins running through the length of both analyzed sections. Despite the very fine-grained texture of Emmaville, suggestive of rapid cooling, the sample has undergone extensive thermal equilibration where larger low-Ca pyroxene grains exhibit coarse exsolution of augite and smaller grains completely recrystallized to low-Ca pyroxene and augite grains ($En_{35}Fs_{61}Wo_4$; $En_{30}Fs_{28}Wo_{42}$) (Fig. 3).

Table 1. Average mineral compositions for Emmaville.

	Pyroxene						Chromite		
	Low Ca	High Ca	Plagioclase		Ilmenite			Low Ti	High Ti
Wt%	n = 111	n = 67	Wt%	n = 130	Wt%	n = 24	Wt%	n = 27	n = 10
SiO_2	48.9	50.8	SiO_2	45.5	TiO_2	51.9	TiO_2	3.3	9.9
TiO_2	0.1	0.2	Al_2O_3	35.3	SiO_2	0.0	SiO_2	0.0	0.1
Al_2O_3	0.8	1.1	FeO	0.4	Cr_2O_3	0.2	Cr_2O_3	50.4	41.3
Cr_2O_3	0.1	0.2	MgO	0.0	Al_2O_3	0.0	Al_2O_3	7.9	5.2
FeO	35.6	16.9	CaO	17.6	V_2O_3	0.1	V_2O_3	0.8	0.7
MnO	1.1	0.5	Na_2O	1.2	FeO	46.2	FeO	35.4	41.1
MgO	11.4	10.1	K_2O	0.1	MnO	0.9	MnO	0.7	0.7
CaO	1.8	19.7	Total	100.1	MgO	0.5	MgO	0.4	0.4
Total	99.7	99.5	An%	88.5	CaO	0.2	CaO	0.2	0.1
Fe/Mn	31.7	31.5	Ab%	11.1	Total	100.2	Total	99.1	99.6
Fe/Mg	1.75	0.94	Or%	0.4	Fe/Mn	49.1	Fe/Mn	50.5	56.0
Mg#	36.43	51.58	Si	2.095	Fe/Mg	47.5	Fe/Mg	47.9	52.9
Wo%	3.99	41.92	Al	1.915	Mg#	2.1	Mg#	2.1	1.9
En%	34.98	29.96	Fe	0.014	Ti	0.983	Cr#	81.1	84.1
Fs%	61.04	28.12	Mg	0.000	Si	0.001	Cm%	71.9	58.772
Si	1.968	1.968	Ca	0.866	Cr	0.004	Mc%	1.8	1.971
Ti	0.003	0.005	Na	0.109	Al	0.000	Hc%	16.8	11.076
Al	0.036	0.052	K	0.004	V	0.002	Sp%	0.4	0.372
Cr	0.002	0.006	Total	5.00	Fe	0.974	Uv%	9.1	27.812
Fe	1.198	0.549			Mn	0.020	Ti	0.088	0.272
Mn	0.038	0.017			Mg	0.021	Si	0.002	0.003
Mg	0.687	0.584			Ca	0.006	Cr	1.440	1.187
Ca	0.078	0.818			Total	2.01	Al	0.337	0.224
Total	4.01	4.00					V	0.023	0.021
							Fe	1.069	1.251
							Mn	0.021	0.022
							Mg	0.023	0.024
							Ca	0.008	0.005
							Total	3.01	3.01

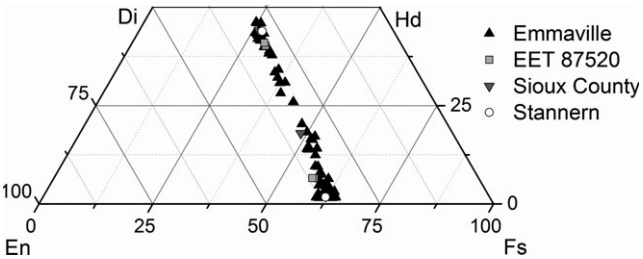

Fig. 3. Truncated pyroxene ternary for Emmaville. Composition data for EET 87520, Sioux County, and Stannern are taken from Mittlefehldt (2015).

Inversion of pigeonite to orthopyroxene typifies type 6 eucrites rather than type 5—the designation of Emmaville given by Takeda and Graham (1991). We suspect that some of the low-Ca pyroxene has inverted to orthopyroxene on the basis of pyroxene compositional data (Table 1). However, it has been shown that low-Ca pyroxene in some basaltic eucrites failed to invert to orthopyroxene and a low-Ca abundance does not necessarily indicate an orthopyroxene crystal structure (see for example, Takeda 1979). Thus, Emmaville may be a type 5 or type 6 eucrite-like basalt.

The plagioclase composition in Emmaville (An_{83-93}) is also similar in composition to typical basaltic eucrites (An_{75-94}; Mittlefehldt [2015] and references therein). The average ilmenite composition of Emmaville (Table 1), is consistent with basaltic eucrite values (TiO_2 = ~52 wt% FeO = ~44 wt%; Mayne et al. 2009; Mittlefehldt 2015), although it can be noted that it is slightly enriched in FeO by ~2 wt%.

Major, Minor, and Trace Elements

Major element compositions are given in Table 2. For all major elements analyzed here, Emmaville plots within a similar range to most basaltic eucrites (SM2). Minor and trace element compositions are given in Table 3. The data presented here are broadly consistent with literature values for these meteorites (see Table S7

Table 2. Bulk major element abundances as measured by ICP-AES.

	Agoult	Camel Donga	Emmaville	Ibitira	Juvinas
Mass (g)	0.02577	0.05	0.02520	0.01357	0.05847
Mg	40.8	44.8	40.2	48.2	40.8
Al	70.2	65.7	66.4	57.7	62.8
K (μg/g)	256	329	363	205	219
Ca	81.8	84.3	82.7	79.9	80.5
Mn	4.40	4.65	4.38	3.86	4.39
Fe	139	145	135	143	133
	Manegaon	Millbillillie	Roda	Sioux County	Tirhert
Mass (g)	0.05824	0.04805	0.04476	0.01499	0.11330
Mg	183	41.9	163	55.2	19.2
Al	9.20	60.6	9.06	38.7	35.1
K (μg/g)	159	347	116	159	178
Ca	12.6	79.0	14.5	68.9	43.5
Mn	3.54	4.44	3.84	5.72	1.92
Fe	118	135	128	210	50.8

All measurements are in mg/g unless otherwise specified.

of Mittlefehldt [2015] and references therein). Cobalt is slightly enriched and bears some similarities to values obtained for diogenites, polymict eucrites, and howardites. In contrast, nickel is an order of magnitude higher than the other basaltic eucrites in this data set (149 ppm as opposed to between 1.46 ppm and 16.3 ppm). The overall REE element pattern for Emmaville is similar to other basaltic eucrites and clearly resolvable from the Stannern trend (Fig. 4). Compared to the other eucrites studied here, Emmaville has high levels of enrichment of Pb (1041 ppb), very slightly elevated abundances of U, Th, and Rb, but with slight depletions in Zr and Hf.

Oxygen Isotopic Composition

Oxygen isotope results are given in Table 4 and plotted in Fig. 5. Also shown in Fig. 5 are the oxygen isotopic analyses for angrites (Greenwood et al. 2005), HEDs (2σ and 3σ from Greenwood et al. 2005, 2014, 2015), the anomalous howardite JaH 556 (Janots et al. 2012), and various anomalous basaltic achondrites (Greenwood et al. 2005, 2013, 2015; Bland et al. 2009; Scott et al. 2009). It is clear from Fig. 5 that Emmaville is an isotopically anomalous eucrite on the basis that its $\Delta^{17}O$ composition lies at least 3σ outside the mean HED value for fall samples ($n = 26$) $\Delta^{17}O = -0.240 \pm 0.021‰$ (3σ) (Greenwood et al. 2016). This is in agreement with the definition of Scott et al. (2009). The mean analyses of the gray (E1) and shock vein-rich (E2) lithologies plot close to the bulk sample (E-B) of Greenwood et al. (2013, 2015, 2016) and have $\Delta^{17}O$ values of $-0.149 \pm 0.012‰$ (2σ) and $-0.160 \pm 0.020‰$ (2σ), respectively (Table 4). In contrast, the light-colored lithology E3 has a somewhat heavier $\Delta^{17}O$ value of $-0.124‰$ and is also significantly heavier with respect to $\delta^{18}O$, that is, 4.873‰ compared to 4.151‰ for E1 and 4.033‰ for E2. The high $\delta^{18}O$ value of E3 together with its light color is consistent with a relative higher feldspar content compared to either E1 or E2 (Table 4).

The combined data for the three Emmaville fractions (E1 + E2 + E3) ($n = 8$) yields an average $\Delta^{17}O$ value of -0.153 ± 0.030 (±2 SD). In comparison, data for 22 diogenites from Greenwood et al. (2014) gave the following average $\Delta^{17}O$ value: -0.246 ± 0.014 (±2 SD). This suggests Emmaville is significantly more heterogeneous than the HED suite. Possible reasons for this higher level of heterogeneity are discussed in further detail below.

DISCUSSION

Mineralogy and Petrology

Primitive bodies in the solar system can have different Fe/Mn ratios in their silicate minerals as a consequence of volatility and oxidation state controls (Papike 1998). Pyroxene Fe/Mn ratios were plotted (Fig. 6) as they contain the bulk of Fe and Mn. Figure 6 shows that the Fe/Mn ratio of Emmaville falls within the normal range of basaltic eucrites and also suggests a common oxidation state for its parental magma.

Chromite grains plot in two discrete groupings within the basaltic eucrite trend (Fig. 7), which represent chromite and a more titanian chromite. To achieve such distinct populations of chromite grains requires different early and late phases of

Table 3. Bulk minor and trace element abundances.

	Agoult	Camel Donga	Emmaville	Ibitira	Juvinas	Manegaon	Millbillillie	Roda	Sioux County	Tirhert
Mass (g)	0.02577	0.05	0.02520	0.01357	0.05847	0.05824	0.04805	0.04476	0.01499	0.11330
Li	10.7	10.1	12.9	7.18	9.99	1.30	12.3	3.35	8.73	4.96
Sc	31.3	39.3	37.4	32.8	31.7	12.8	36.5	25.2	40.8	17.4
Ti (mg/g)	2.90	4.65	4.72	5.49	3.72	0.44	3.59	1.05	3.48	1.57
V	51.4	71.7	65.8	72.5	61.1	114	67.6	93.6	82.0	34.4
Cr (mg/g)	1.20	2.03	1.85	2.63	1.53	5.25	1.90	3.16	2.18	0.93
Co	6.19	8.07	14.8	9.00	5.76	16.7	6.71	27.38	7.13	3.20
Ni	1.46	16.3	149	5.74	1.05	28.3	1.60	35.5	1.29	0.38
Cu	0.95	1.25	3.31	1.03	9.83	4.45	3.21	13.0	0.45	0.17
Zn	1.06	1.57	3.06	2.11	3.31	2.09	2.53	2.99	2.81	0.38
Ga	1.77	1.47	2.06	0.99	1.70	0.25	1.55	0.38	1.02	1.00
Rb (ng/g)	116	243	712	114	139	77.5	460	105	103	81.5
Sr	82.5	84.4	89.1	78.9	77.7	7.80	74.1	5.6	47.2	44.1
Y	12.6	21.9	24.0	20.8	18.1	1.28	17.7	3.42	14.5	8.08
Zr	26.1	53.5	41.1	54.9	40.6	3.41	29.6	7.51	28.4	22.2
Ba	30.2	33.8	37.9	33.8	29.8	1.94	33.1	4.00	16.4	14.9
La	1.11	3.30	3.66	3.31	2.81	0.18	2.83	0.25	1.44	1.41
Ce	2.81	7.99	9.22	8.05	6.51	0.44	6.55	0.61	3.74	3.45
Pr	0.44	1.24	1.41	1.25	1.00	0.07	1.02	0.10	0.59	0.53
Nd	2.33	6.27	7.23	6.27	5.08	0.37	5.20	0.53	3.19	2.66
Sm	0.91	2.12	2.38	2.06	1.69	0.13	1.76	0.21	1.14	0.86
Eu	0.65	0.70	0.75	0.65	0.60	0.05	0.61	0.05	0.38	0.35
Gd	1.28	2.72	3.04	2.66	2.19	0.16	2.25	0.35	1.60	1.09
Tb	0.27	0.53	0.58	0.51	0.42	0.03	0.44	0.08	0.34	0.20
Dy	1.88	3.41	3.74	3.32	2.68	0.20	2.82	0.54	2.28	1.30
Ho	0.44	0.77	0.83	0.74	0.60	0.04	0.64	0.13	0.52	0.29
Er	1.44	2.38	2.52	2.32	1.91	0.15	2.08	0.43	1.68	0.90
Yb	1.45	2.09	2.20	2.07	1.61	0.13	1.76	0.44	1.69	0.78
Lu	0.23	0.32	0.33	0.32	0.24	0.02	0.26	0.07	0.26	0.11
Hf	0.80	1.53	0.77	1.57	1.16	0.10	1.05	0.25	0.84	0.65
Pb (ng/g)	165	272	1041	265	246	581	722	452	195	161
Th (ng/g)	121	437	487	385	358	21.9	404	33.55	213	197
U (ng/g)	49.4	82.9	121.7	90.3	68.3	6.72	114	11.7	69.8	42.1

All measurements are in μg/g unless otherwise specified.

crystallization. Elemental abundances of Cr and Ti in chromite have been linked to different degrees of oxidation, with Cr more abundant in reduced conditions and greater abundances of Ti in more oxidizing conditions (Bunch and Keil 1971); it is therefore possible that the two populations of chromite grains are linked to a change in the oxidation state of the parental melt. High-Ti chromite grains are also a typical feature of highly metamorphosed eucrites owing to the decomposition of ulvöspinel (Yamaguchi et al. 2001, 2002, 2009). These Ti-rich chromite grains are typically found in close association with ilmenite, something not commonly observed in Emmaville.

Major and Trace Elements

The major element abundances for Emmaville are similar to those published in the literature (Mason 1974; Stolper 1977). The depletion of Hf and Zr could in principle be caused by an incomplete dissolution of zircons. As all of the samples presented here underwent the same acid digestion protocol, if partial digestion of zircon occurred it is likely that other samples would be similarly affected. Given the lack of evidence for partial zircon dissolution in the basaltic eucrite Camel Donga, which yields Zr and Hf abundances consistent with literature values (Cleverly et al. 1986; Palme et al. 1988; Barrat et al. 2000), it is unlikely that Emmaville would have been affected. Another possibility which fits with the mineralogical data is that zircon grains are rare within the Emmaville eucrite and could potentially be under-represented within the powdered sample. When compared to the Zr and Hf abundances of the anomalous achondrite Bunburra Rockhole (Spivak-Birndorf et al. 2015), Emmaville displays

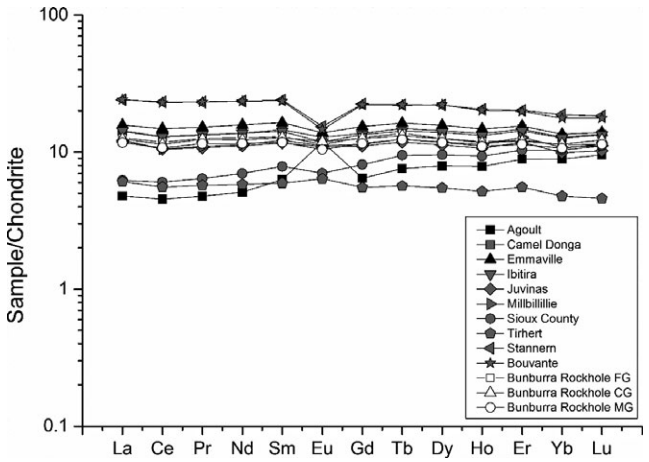

Fig. 4. REE pattern of Emmaville, anomalous eucrites, Bunburra Rockhole, and Ibitira along with representative eucrites. Published values for Bouvante and Stannern are from Barrat et al. (2007). Data for Bunburra Rockhole are taken from Spivak-Birndorf et al. (2015) and follow the same abbreviation style, whereby FG, MG, and CG correspond to the fine-, medium-, and coarse-grained domains outlined in the publication. The reference chondrite is from Lodders (2003).

similar abundances for both elements, albeit at slightly lower concentrations (Zr = 41.1 ppm compared to Bunburra Rockhole's ~45 ppm).

The eucrite Sioux County in Fig. 4 is depleted in LREEs with an increase in abundance toward the heavier REEs. This could be due to the coarse-grained nature of the eucrite and reflect heterogeneity in the powdered sample used in this study with respect to REE-rich phases such as apatite. Tirhert is also a very coarse-grained eucrite, however, in the case of this meteorite, the REE pattern is flatter with a small depletion toward the HREEs. While no preferential depletion of LREEs is observed it may still be possible that the low abundances of REEs reflect a heterogeneous powder under-represented in the REE carrying phases such as Ca-phosphate.

The achondrite Bunburra Rockhole shares several similarities with Emmaville in terms of its major element, REEs, and oxygen isotope signature (Spivak-Birndorf et al. 2015). As a result of these similarities, in particular the similar oxygen isotope signature, we speculate that these two meteorites share a common parent body. The modal mineralogy of Bunburra Rockhole falls on the trend line defined by pyroxene versus plagioclase modal abundance for eucrites (Fig. 8). However, Emmaville lies off this trend, plotting below the pyroxene-plagioclase trend of basaltic eucrites on account of the large amount of quartz observed in our sample. Despite this, both share similar mineralogies and Fe/Mn ratios of pyroxene with noncumulate eucrites. Trace element data for these two meteorites are also comparable to typical eucrites. However, as noted before, the elevated Ni abundance of Emmaville (Table 3) is in stark contrast to Bunburra Rockhole, which is depleted in Ni relative to most eucrites (Spivak-Birndorf et al. 2015). This is particularly surprising as the most likely mineral to host Ni in Emmaville is pyroxene, which has a lower modal abundance compared to typical basaltic eucrites and Bunburra rockhole. This could be attributed to a greater amount of Ni partitioning into the core of the anomalous eucrite parent body, or different initial abundances between eucrites and Bunburra Rockhole (Spivak-Birndorf et al. 2015). Cobalt in Emmaville is also enriched compared to basaltic eucrites and Bunburra Rockhole. The enrichment of Co and Ni abundance in Emmaville is difficult to reconcile with a similar Co abundance and depletion of Ni observed in Bunburra Rockhole if they are thought to originate from the same parent body.

The Co abundance of Emmaville is similar to diogenites, polymict eucrites, and howardites. This could imply that Emmaville has undergone some impact mixing, however, based on the petrography and element maps conducted on the sections and melt veins studied here, we find no evidence for mixing with diogenitic or chondritic material. Another possible indication of impact mixing is elevated siderophile elements such as Ni. To eliminate this possibility, the percentage of impactor material needed to elevate a typical eucrite to the Ni and O isotope values observed in this study was modeled for both H and L chondrites. Ni contents of 16000 ppm and 12000 ppm were used for H and L chondrites, respectively (Wasson and Kallemeyn 1988), a Ni content of 2.3 ppm for pristine noncumulate eucrites (Warren et al. 2009) and $\Delta^{17}O$ values from Clayton et al. (1991) and Greenwood et al. (2016). It was found that ~1% H or L chondrite material was required to elevate Ni to comparable levels but did not elevate $\Delta^{17}O$ significantly. To reconcile the O isotopes with impactor material ~10% mixing is required; however, this results in approximately an order of magnitude more Ni than observed. This further strengthens our conclusion that Emmaville has not had significant impact contamination.

Oxygen Isotopes

The majority of diogenite, eucrite, and cumulate eucrite samples have virtually identical $\Delta^{17}O$ values (Fig. 1) (Scott et al. 2009; Greenwood et al. 2014). This has been cited as evidence to support the view that all of the major HED lithologies are derived from a single, isotopically homogeneous parent asteroid, widely believed to be Vesta (Greenwood et al. 2005; McSween et al. 2013). However, as pointed out by Scott et al.

Table 4. Oxygen isotope composition of different lithologies in Emmaville.

Sample	Comments	N	$\delta^{17}O‰$	2 × SD	2 × SEM	$\delta^{18}O‰$	2 × SD	2 × SEM	$\Delta^{17}O‰$	2 × SD	2 × SEM
Emmaville E1	Dull gray homogeneous lithology	2	2.027	0.112	0.079	4.151	0.190	0.134	−0.149	0.012	0.009
Emmaville E2	Shock vein-rich fraction	5	1.954	0.076	0.034	4.033	0.159	0.071	−0.160	0.020	0.009
Emmaville E3	"Light-colored" lithology	1	2.430			4.873			−0.124		
Emmaville E1 + E2 + E3	Overall average of 8 replicates	8	2.032	0.336	0.119	4.168	0.597	0.211	−0.153	0.030	0.011
Obsidian Standard*		39	3.808	0.052	0.008	7.267	0.093	0.015	0.001	0.017	0.003

*Obsidian standard values taken from Starkey et al. (2016)

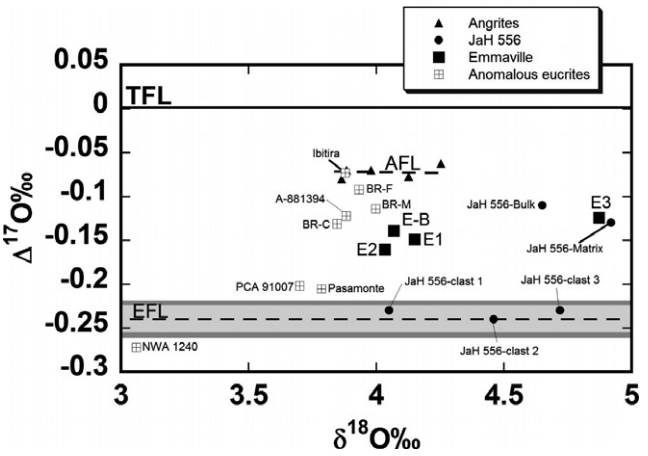

Fig. 5. Oxygen isotopic composition of Emmaville compared to HEDs, angrites, and anomalous basaltic achondrites. Light gray shading = ±2σ variation in mean HED $\Delta^{17}O$ value, Dark gray shading = ± 3σ variation in mean HED $\Delta^{17}O$ value (see text for further discussion). Abbreviations: TFL: terrestrial fractionation line, AFL: angrite fractionation line (Greenwood et al. 2005), BR-F, BR-M, BR-C: fine, medium, and coarse fractions from Bunburra Rockhole (Bland et al. 2009); E-B: Emmaville bulk (Greenwood et al. 2013, 2016); E-1, E-2, E-3: Emmaville fractions in this study (see text for further details). Analyses of PCA 91007, Pasamonte, and A-881394, NWA 1240 (Scott et al. 2009), Ibitira (Greenwood et al. 2016), and JaH 556 (Janots et al. 2012).

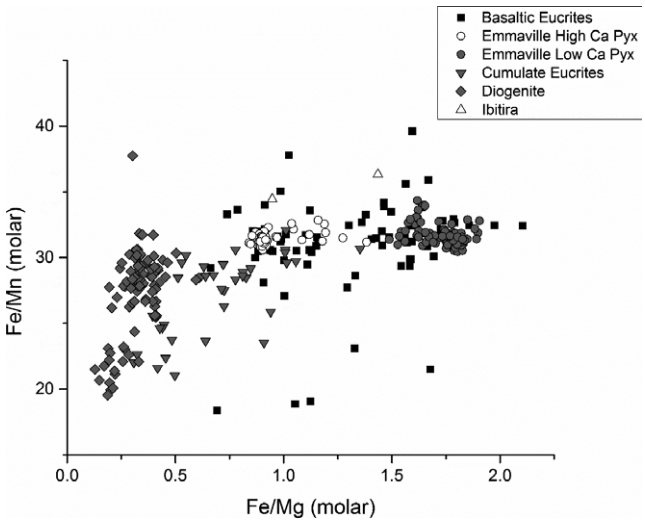

Fig. 6. Pyroxene Fe/Mn versus Fe/Mg diagram. Basaltic eucrite, cumulate eucrite, diogenite, and Ibitira data taken from Mittlefehldt (2015).

(2009), a relatively small group of basaltic achondrites (Fig. 5) have $\Delta^{17}O$ that lie at least 3σ outside the mean value defined by the HED falls, that is, −0.240 ± 0.021‰ (3σ) (n = 26) (Greenwood et al. 2016). With the exception of NWA 1240 (Scott et al. 2009) and NWA 011 (Yamaguchi et al. 2002) (not shown in Fig. 5) all of the presently identified anomalous basaltic achondrites plot between the eucrite fractionation line (EFL) and the angrite fractionation line (AFL) on Fig. 5.

As pointed out by McSween et al. (2013), various scenarios have been envisaged to explain the origin of these isotopically anomalous basaltic achondrites and will be discussed later. One such scenario proposed by Wiechert et al. (2004) is that both normal and anomalous samples come from a single heterogeneous HED parent body based on the variation of ^{16}O observed in certain HEDs. In contrast, Scott et al. (2009) suggested that the isotopically anomalous samples may have come from distinct asteroidal sources. This latter explanation implies that the HED parent body itself had a very homogeneous $\Delta^{17}O$ composition, consistent with magma ocean models for Vesta (Righter and Drake 1997; Greenwood et al. 2005). As an explanation for the origin of at least some anomalous basaltic achondrites, Greenwood et al. (2005) and Janots et al. (2012) highlighted the possible role of impact processes as a mechanism for producing isotopic heterogeneity.

For a few anomalous eucrites such as Ibitira (Wiechert et al. 2004; Mittlefehldt 2005), A-881394

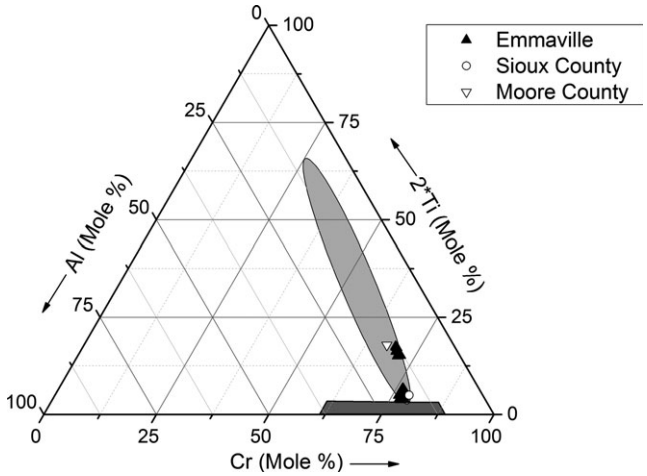

Fig. 7. Chromite ternary diagram. The light gray ellipse represents variations with basaltic eucrites, the darker gray box represents variations within the diogenites. Data are from Bunch and Keil (1971), Mittlefehldt (1994), and Mittlefehldt (2015).

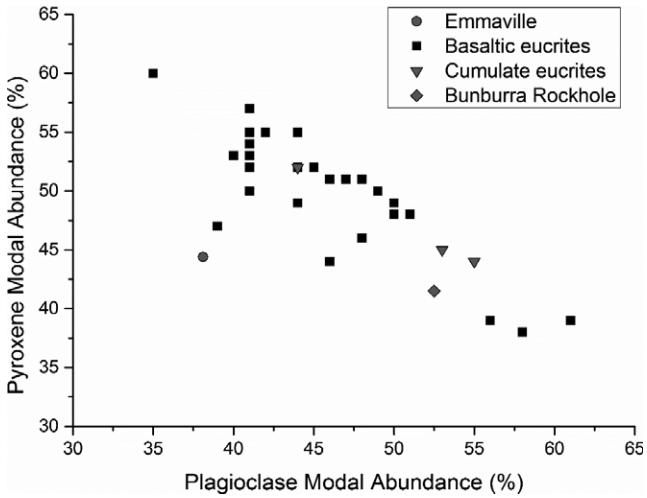

Fig. 8. A comparison of the relative modal abundances of plagioclase and pyroxene in eucrites after Mayne et al. (2009). Bunburra Rockhole data are taken from Spivak-Birndorf et al. (2015).

(Nyquist et al. 2003), and the anomalous achondrite NWA 011 (Yamaguchi et al. 2002) a range of evidence would suggest that they are not from the same parent body as the majority of HED samples (Scott et al. 2009). However, the situation is less clear cut for the other anomalous eucrites, with at least some showing significant degrees of brecciation (e.g., Pasamonte; Metzler et al. 1995). The tightly constrained O-isotope distribution of anomalous basaltic meteorites (with the notable exception of NWA 011), lying between the EFL and AFL (Fig. 5) could be interpreted as supporting an origin by impact mixing between HED lithologies and material that lies above the AFL (i.e., with an isotopic composition that may be similar to that of the ordinary chondrites). A clear example of where this has actually taken place is provided by the anomalous howardite JaH 556 (Janots et al. 2012).

JaH 556 is a weathered impact melt breccia, comprising highly shocked clasts set in a finely recrystallized vesicular matrix. The bulk oxygen isotope composition of JaH 556 is anomalous, with a $\Delta^{17}O$ value of $-0.11‰$ (Fig. 5). In contrast, EATG (ethanolamine thioglycolate)-washed clasts in JaH 556 have normal HED $\Delta^{17}O$ values (Fig. 5). JaH 556 has a highly enriched siderophile element content and contains clasts that appear to be relict chondrules, with olivine compositions consistent with an H chondrite precursor. Both the siderophile element content and bulk oxygen isotope composition of JaH 556 point to admixing of a 10–15% H chondrite component in this meteorite. An impact origin for an anomalous HED could be overlooked in the case where a lower percentage of impactor material is present, or was non-chondritic (i.e., low siderophile element content).

Unlike JaH 556, none of the various fractions separated from Emmaville (E1, E2, E3) plot close to the EFL (Fig. 5). Emmaville also has a basaltic eucrite mineralogy and mineral compositions, and the element maps show no clear evidence of any exogenous material. Any incorporated material would also likely have affected the bulk major and trace elements, a feature not reflected in the majority of our data as discussed above. Another possibility is that the impact of an isotopically distinct body onto Vesta during the late stages of magma ocean crystallization could have resulted in isotopically distinct basalts. The petrologic model of Mandler and Elkins-Tanton (2013) invokes continuous or periodic recharge of shallow magma chambers by residual melts derived from deeper in the solidifying mantle as a means to produce the observed suite of HED lithologies. An impact at this stage could produce a regional difference in O isotopic signature in the magma that was not homogenized through the body. Impact contaminated basalts, however, would likely have differing compositions to normal basaltic eucrites depending on the amount of exogenous material incorporated into their parental melt. For anomalous eucrites such as Ibitira or Pasamonte to be from Vesta, they would both require different, as yet unknown, types of impactor contamination (Wiechert et al. 2004; Scott et al. 2009). This evidence would appear to exclude the possibility that Emmaville represents a howardite-like impact breccia composed of projectile material with a $\Delta^{17}O$ composition lying above the AFL that was mixed with isotopically normal HED material. Instead, Emmaville more closely resembles the

case of Bunburra Rockhole (Bland et al. 2009; Benedix et al. 2014) in which there is evidence of some isotopic heterogeneity, but none of the various fractions have a HED $\Delta^{17}O$ composition. Although the various fractions of Emmaville are slightly displaced to lighter $\Delta^{17}O$ values than Bunburra Rockhole there would appear to be considerable overlap between the two meteorites, based on a comparison of O isotopes between Fig. 5 of this study and Fig. 1 of Benedix et al. (2014). Benedix et al. (2014) suggested that Bunburra Rockhole may be derived from the same parent body as A-881394. If this interpretation is correct then Emmaville may represent a third sample from this body.

Possible Parent Bodies for the Emmaville Eucrite

With mineral compositions and REEs indistinguishable from ordinary basaltic eucrites and an impactor component unlikely, there are two explanations to reconcile the difference in O isotopes with that of normal HEDs. The two possible explanations are:

1. The HED parent body is not as well homogenized as was previously considered (Wiechert et al. 2004; Greenwood et al. 2005, 2014; Scott et al. 2009).
2. Emmaville is from a separate parent body which produced basalts of similar composition to the eucrites of the HED clan (Scott et al. 2009).

The HED parent body, Vesta, is believed to have differentiated with a well-mixed magma ocean which should have homogenized the various isotopic systems (Righter and Drake 1997; Greenwood et al. 2005; Mandler and Elkins-Tanton 2013). If this magma ocean was not as well mixed as previously expected it is possible that the isotope systematics may not have fully equilibrated. In this scenario, basalts derived from different regions would still be similar in chemical composition, as they derived from the same starting material, but their isotopic systematics would reflect the degree of local equilibration (Wiechert et al. 2004). Ghosh and McSween (1998) suggested that the outer layers of Vesta could have retained some isotopic heterogeneity and never reached the melting temperature to become equilibrated. Their model not only still predicts the perfect homogenization of the interior of Vesta but also allows some oxygen isotope heterogeneity. One problem with this idea, however, is that the outer layers are likely to have been assimilated into the Vestan mantle owing to differences in density (Mandler and Elkins-Tanton 2013).

The argument for a heterogeneous Vesta encounters several problems, predominant among which is the striking homogeneity of the majority of HED meteorites. Impacts have excavated the HED parent body to significant depth and to date, only the highly shocked diogenite Dhofar 778 (shock stage S4) has an anomalous oxygen isotope composition (Greenwood et al. 2016). It is possible, however, that most of the HEDs currently available could have been excavated from a single impact event (Bogard and Garrison 2003), as these smaller groups of eucrites with differing O isotopes may well represent material excavated from different areas across the surface of Vesta.

Bunburra Rockhole, A-881394, Elephant Moraine (EET) 92023, and Emmaville are all distinct in oxygen isotope composition despite being similar in petrology and mineral compositions to that of the HED parent body. Variations in $\varepsilon^{54}Cr$ have also previously been used to identify meteorite groups or parent bodies (e.g., Trinquier et al. 2007; Qin et al. 2010). On a plot of $\Delta^{17}O$ versus $\varepsilon^{54}Cr$ both A-881394 and Bunburra Rockhole form a distinct cluster that is fully resolvable from normal eucrites (Benedix et al. 2014). Although the $\varepsilon^{54}Cr$ composition of Emmaville and EET 92023 have not yet been determined, on the basis of their similar oxygen isotope compositions it seems possible that all four samples (Bunburra Rockhole, A-881394, Emmaville, and EET 92023) are derived from an isotopically distinct HED-like parent. It is, on the other hand, possible for these meteorites to not all be derived from a single parent body as the similarities in O isotopic composition do not necessarily imply a genetic relationship. Recent preliminary petrologic data by Mittlefehldt et al. (2016), as part of an ongoing campaign, suggests that A-881394 and EET 92023 may well be from separate asteroids in spite of their similar O isotopic composition. These petrological differences preclude these four meteorites forming a grouplet as defined by Weisberg et al. (2006).

CONCLUSIONS

We conclude the following based on our studies:

1. Mineral compositions of Emmaville are consistent with basaltic eucrites
2. Bulk major, minor, and trace elements are consistent with basaltic eucrites
3. Oxygen isotopes of separated lithologies of Emmaville are heterogeneous where the dark gray and shocked lithologies plot near the bulk composition and the light gray lithology being slightly enriched in $\delta^{17}O$ and significantly enriched in $\delta^{18}O$
4. Oxygen isotopes for the majority of Emmaville plot in a similar region to Bunburra Rockhole, A-881394, and EET 92023
5. Either Vesta is more heterogeneous than previously thought in terms of O isotopes or Emmaville originates from a separate parent body which had a similar composition and evolutionary history.

Our results provide a detailed account of the mineralogy as well as bulk chemistry of the Emmaville eucrite, and suggest that it is nearly indistinguishable from basaltic eucrites in terms of mineralogy and bulk composition, but its oxygen isotopes and fine-grained metamorphic texture stand out as anomalous. This study presents three hypotheses for the formation of this anomalous eucrite and although its origin is still uncertain, the differences in oxygen isotope composition coupled with evidence against a heterogeneous Vesta or obvious impactor contamination lead us to conclude it is more plausible that Emmaville is from a separate parent body.

ACKNOWLEDGMENTS

This work was funded in part by STFC for studentship and the Royal Astronomical Society (to TJB) and the NASA Cosmochemistry and Emerging Worlds Programs (to DWM). Oxygen isotope work was funded by STFC awarded to IAF (Grant ST/1001964/1). We thank Caroline Smith at the Natural History Museum, London UK and Linda Welzenbach at the Smithsonian Institution for samples without which this work would not be possible. Special thanks are given to Ross Pogson at the Australian Museum for sample chips without which this project could not have been undertaken. Thanks go to Patrick Rafferty for help with the ICP-AES at the Open University and Peter Landsberg for help with the interpretation. The reviewers N. G. Lunning and N. Shirai, along with associate editor A. Yamaguchi and Editor Timothy Jull are thanked for their constructive comments.

Editorial Handling—Dr. Akira Yamaguchi

REFERENCES

Barrat J., Blichert-Toft J., Gillet P., and Keller F. 2000. The differentiation of eucrites: The role of in situ crystallization. *Meteoritics & Planetary Science* 35:1087–1100.

Barrat J., Yamaguchi A., Greenwood R., Bohn M., Cotten J., Benoit M., and Franchi I. 2007. The Stannern trend eucrites: Contamination of main group eucritic magmas by crustal partial melts. *Geochimica et Cosmochimica Acta* 71:4108–4124.

Benedix G., Bland P., Friedrich J., Mittlefehldt D., Sanborn M., Yin Q.-Z., Greenwood R., Franchi I., Bevan A., and Towner M. 2014. Bunburra rockhole: Exploring the geology of a new differentiated basaltic asteroid (abstract #1650). 45th Lunar and Planetary Institute Science Conference. CD-ROM.

Bland P. A., Spurný P., Towner M. C., Bevan A. W. R., Singleton A. T., Bottke W. F., Greenwood R. C., Chesley S. R., Shrbený L., Borovička J., Ceplecha Z., McClafferty T. P., Vaughan D., Benedix G. K., Deacon G., Howard K. T., Franchi I. A., and Hough R. M. 2009. An anomalous basaltic meteorite from the innermost main belt. *Science* 325:1525–1527.

Bogard D. D. and Garrison D. H. 2003. 39Ar-40Ar ages of eucrites and thermal history of asteroid 4 Vesta. *Meteoritics & Planetary Science* 38:669–710.

Bunch T. and Keil K. 1971. Chromite and ilmenite in nonchondritic meteorites (Chromite and ilmenite analysis in pallasites, mesosiderites, achondrites and meteorites with electron microprobe). *American Mineralogist* 56:146–157.

Clayton R. N., Mayeda T. K., Goswami J. N., and Olsen E. J. 1991. Oxygen isotope studies of ordinary chondrites. *Geochimica et Cosmochimica Acta* 55:2317–2337.

Cleverly W., Jarosewich E., and Mason B. 1986. Camel Donga meteorite, a new eucrite from the Nullarbor Plain, Western Australia. *Meteoritics* 21:263–269.

Eggins S. M., Woodhead J. D., Kinsley L. P. J., Mortimer G. E., Sylvester P., McCulloch M. T., Hergt J. M., and Handler M. R. 1997. A simple method for the precise determination of ≥ 40 trace elements in geological samples by ICPMS using enriched isotope internal standardisation. *Chemical Geology* 134:311–326.

Floss C., Taylor L. A., Promprated P., and Rumble D. 2005. Northwest Africa 011: A "eucritic" basalt from a non-eucrite parent body. *Meteoritics & Planetary Science* 40:343–360.

Ghosh A. and McSween H. Y. 1998. A thermal model for the differentiation of asteroid 4 Vesta, based on radiogenic heating. *Icarus* 134:187–206.

Greenwood R. C., Franchi I. A., Jambon A., and Buchanan P. C. 2005. Widespread magma oceans on asteroidal bodies in the early solar system. *Nature* 435:916–918.

Greenwood R. C., Barrat J.-A., Scott E., Janots E., Franchi I., Hoffman B., Yamaguchi A., and Gibson J. 2012. Has Dawn gone to the wrong asteroid? Oxygen isotope constraints on the nature and composition of the HED parent body (abstract #2271). 43rd Lunar and Planetary Science Conference. CD-ROM.

Greenwood R. C., Barrat J., Scott E. R. D., Franchi I. A., Yamaguchi A., Gibson J., Haack H., Lorenz C., Ivanova M. A., and Bevan A. 2013. Large-scale melting and impact mixing on early-formed asteroids: Evidence from high-precision oxygen isotope studies (abstract #3048). 44th Lunar and Planetary Institute Science Conference. CD-ROM.

Greenwood R. C., Barrat J.-A., Yamaguchi A., Franchi I. A., Scott E. R. D., Bottke W. F., and Gibson J. M. 2014. The oxygen isotope composition of diogenites: Evidence for early global melting on a single, compositionally diverse, HED parent body. *Earth and Planetary Science Letters* 390:165–174.

Greenwood R. C., Barrat J.-A., Scott E. R. D., Haack H., Buchanan P. C., Franchi I. A., Yamaguchi A., Johnson D., Bevan A. W. R., and Burbine T. H. 2015. Geochemistry and oxygen isotope composition of main-group pallasites and olivine-rich clasts in mesosiderites: Implications for the "great dunite shortage" and HED-mesosiderite connection. *Geochimica et Cosmochimica Acta* 169:115–136.

Greenwood R. C., Burbine T. H., Miller M. F., and Franchi I. A. 2016. Melting and differentiation of early-formed asteroids: The perspective from high precision oxygen isotope studies. *Chemie der Erde – Geochemistry*, doi:10.1016/j.chemer.2016.09.005

Janots E., Gnos E., Hofmann B., Greenwood R., Franchi I., Bermingham K., and Netwing V. 2012. Jiddat al Harasis 556: A howardite impact melt breccia with an H chondrite component. *Meteoritics & Planetary Science* 47:1558–1574.

Lodders K. 2003. Solar system abundances and condensation temperatures of the elements. *The Astrophysical Journal* 591:1220.

Mandler B. E. and Elkins-Tanton L. T. 2013. The origin of eucrites, diogenites, and olivine diogenites: Magma ocean crystallization and shallow magma chamber processes on Vesta. *Meteoritics & Planetary Science* 48:2333–2349.

Mason B. 1974. Notes on Australian meteorites. *Records of the Australian Museum* 29:169–186.

Mayne R., McSween H., McCoy T., and Gale A. 2009. Petrology of the unbrecciated eucrites. *Geochimica et Cosmochimica Acta* 73:794–819.

McSween H. Y., Binzel R. P., De Sanctis M. C., Ammannito E., Prettyman T. H., Beck A. W., Reddy V., Le Corre L., Gaffey M. J., McCord T. B., Raymond C. A., Russell C. T., and the Dawn Science T. 2013. Dawn; the Vesta–HED connection; and the geologic context for eucrites, diogenites, and howardites. *Meteoritics & Planetary Science* 48:2090–2104.

Metzler K., Bobe K., Palme H., Spettel B., and Stöffler D. 1995. Thermal and impact metamorphism on the HED parent asteroid. *Planetary and Space Science* 43:499–525.

Miller M. F. 2002. Isotopic fractionation and the quantification of ^{17}O anomalies in the oxygen three-isotope system: An appraisal and geochemical significance. *Geochimica et Cosmochimica Acta* 66:1881–1889.

Miller M., Franchi I., Sexton A., and Pillinger C. 1999. High-precision δ17O isotope measurements of oxygen from silicates and other oxides: Method and applications. *Rapid Communications in Mass Spectrometry* 13:1211–1217.

Mittlefehldt D. W. 1994. The genesis of diogenites and HED parent body petrogenesis. *Geochimica et Cosmochimica Acta* 58:1537–1552.

Mittlefehldt D. W. 2005. Ibitira: A basaltic achondrite from a distinct parent asteroid and implications for the Dawn mission. *Meteoritics & Planetary Science* 40:665–677.

Mittlefehldt D. W. 2015. Asteroid 4 Vesta: I. The howardite-eucrite-diogenite (HED) clan of meteorites. *Chemie der Erde—Geochemistry* 75:155–183.

Mittlefehldt D. W., Greenwood R. C., Peng Z. X., Ross D. K., Berger E. L., and Barrett T. J. 2016. Petrologic and oxygen-isotopic investigation of eucritic and anomalous mafic achondrites (abstract #1240). 47th Lunar and Planetary Science Conference. CD-ROM.

Morgan J. W. and Lovering J. F. 1973. Uranium and thorium in achondrites. *Geochimica et Cosmochimica Acta* 37:1697–1707.

Nyquist L., Reese Y., Wiesmann H., Shih C.-Y., and Takeda H. 2003. Fossil 26 Al and 53 Mn in the Asuka 881394 eucrite: Evidence of the earliest crust on asteroid 4 Vesta. *Earth and Planetary Science Letters* 214:11–25.

Palme H., Wlotzka F., Spettel B., Dreibus G., and Weber H. 1988. Camel Donga: A eucrite with high metal content. *Meteoritics* 23:49–57.

Papike J. J. 1998. Comparative planetary mineralogy: Chemistry of melt-derived pyroxene, feldpar and olivine. In *Planetary materials*, edited by Papike J. J. Washington, D. C.: Mineralogical Society of America. pp. 7-1–7-11.

Qin L., Alexander C. M. O'D., Carlson R. W., Horan M. F., and Yokoyama T. 2010. Contributors to chromium isotope variation of meteorites. *Geochimica et Cosmochimica Acta* 74:1122–1145.

Righter K. and Drake M. J. 1997. A magma ocean on Vesta: Core formation and petrogenesis of eucrites and diogenites. *Meteoritics & Planetary Science* 32:929–944.

Rogers N. W., Thomas L. E., Macdonald R., Hawkesworth C. J., and Mokadem F. 2006. ^{238}U–^{230}Th disequilibrium in recent basalts and dynamic melting beneath the Kenya rift. *Chemical Geology* 234:148–168.

Scott E. R. D., Greenwood R. C., Franchi I. A., and Sanders I. S. 2009. Oxygen isotopic constraints on the origin and parent bodies of eucrites, diogenites, and howardites. *Geochimica et Cosmochimica Acta* 73:5835–5853.

Spivak-Birndorf L. J., Bouvier A., Benedix G. K., Hammond S., Brennecka G. A., Howard K., Rogers N., Wadhwa M., Bland P. A., Spurný P., and Towner M. C. 2015. Geochemistry and chronology of the Bunburra Rockhole ungrouped achondrite. *Meteoritics & Planetary Science* 50:958–975.

Starkey N. A., Jackson C. R. M., Greenwood R. C., Parman S., Franchi I. A., Jackson M., Fitton J. G., Stuart F. M., Kurz M., and Larsen L. M. 2016. Triple oxygen isotopic composition of the high-3He/4He mantle. *Geochimica et Cosmochimica Acta* 176:227–238.

Stolper E. 1977. Experimental petrology of eucritic meteorites. *Geochimica et Cosmochimica Acta* 41:587–611.

Takeda H. 1979. A layered-crust model of a Howardite parent body. *Icarus* 40:455–470.

Takeda H. and Graham A. 1991. Degree of equilibration of eucritic pyroxenes and thermal metamorphism of the earliest planetary crust. *Meteoritics* 26:129–134.

Trinquier A., Birck J. L., and Allègre C. J. 2007. Widespread ^{54}Cr heterogeneity in the inner solar system. *The Astrophysical Journal* 655:1179.

Warren P. H., Kallemeyn G. W., Huber H., Ulff-Møller F., and Choe W. 2009. Siderophile and other geochemical constraints on mixing relationships among HED-meteoritic breccias. *Geochimica et Cosmochimica Acta* 73:5918–5943.

Wasson J. and Kallemeyn G. 1988. Compositions of chondrites. *Philosophical Transactions of the Royal Society of London A: Mathematical, Physical and Engineering Sciences* 325:535–544.

Weisberg M. K., McCoy T. J., and Krot A. N. 2006. Systematics and evaluation of meteorite classification. In *Meteorites and the early solar system II*, edited by Lauretta D. S. and McSween H. Y. Tucson, Arizona: University of Arizona Press. pp. 19–52.

Wiechert U. H., Halliday A. N., Palme H., and Rumble D. 2004. Oxygen isotope evidence for rapid mixing of the HED meteorite parent body. *Earth and Planetary Science Letters* 221:373–382.

Yamaguchi A., Taylor G. J., and Keil K. 1996. Global crustal metamorphism of the eucrite parent body. *Icarus* 124:97–112.

Yamaguchi A., Taylor G. J., Keil K., Floss C., Crozaz G., Nyquist L. E., Bogard D. D., Garrison D. H., Reese Y. D., Wiesmann H., and Shih C. Y. 2001. Post-crystallization reheating and partial melting of eucrite EET 90020 by impact into the hot crust of asteroid 4Vesta ~4.50 Ga ago. *Geochimica et Cosmochimica Acta* 65:3577–3599.

Yamaguchi A., Clayton R. N., Mayeda T. K., Ebihara M., Oura Y., Miura Y. N., Haramura H., Misawa K., Kojima H., and Nagao K. 2002. A new source of basaltic

meteorites inferred from Northwest Africa 011. *Science* 296:334–336.
Yamaguchi A., Barrat J. A., Greenwood R. C., Shirai N., Okamoto C., Setoyanagi T., Ebihara M., Franchi I. A., and Bohn M. 2009. Crustal partial melting on Vesta: Evidence from highly metamorphosed eucrites. *Geochimica et Cosmochimica Acta* 73:7162–7182.

SUPPORTING INFORMATION

Additional supporting information may be found in the online version of this article:

Data S1: Standard values and associated errors
Data S2: Confirmation of mineral quartz via Raman spectroscopy